

Surround-gated vertical nanowire quantum dots

M. H. M. van Weert,¹ M. den Heijer,¹ M. P. van Kouwen,¹ R. E. Algra,^{2,a)}
E. P. A. M. Bakkers,^{1,b)} L. P. Kouwenhoven,¹ and V. Zwiller^{1,c)}

¹Kavli Institute of Nanoscience, Delft University of Technology, Delft, Zuid Holland 2628CJ, The Netherlands

²Philips Research Eindhoven, Eindhoven, Noord Brabant 5600AE, The Netherlands

(Received 5 May 2010; accepted 14 May 2010; published online 11 June 2010)

We report voltage dependent photoluminescence experiments on single indium arsenide phosphide (InAsP) quantum dots embedded in vertical surround-gated indium phosphide (InP) nanowires. We show that by tuning the gate voltage, we can access different quantum dot charge states. We study the anisotropic exchange splitting by polarization analysis, and identify the neutral and singly charged exciton. These results are important for spin addressability in a charge tunable nanowire quantum dot. © 2010 American Institute of Physics. [doi:10.1063/1.3452346]

Optically active quantum dots are sources for single¹ and entangled² photons and allow for single electron charging.³ These properties make them highly interesting for quantum information processing.⁴ Recently, initialization,^{5,6} manipulation,^{7,8} and readout of single spins have been demonstrated experimentally in such systems. Semiconducting nanowires possess an unprecedented material and design freedom,⁹ and offer the possibility of combining optically active quantum dots^{10,11} with electrostatically defined quantum dots,¹² which would allow for the combination of local electron spin manipulation in the electrostatically defined dot and fast optical readout via the optically active quantum dot. Nanowire quantum dots have excellent optical quality,¹³ and allow for electron charging down to the single electron level.¹⁴ The proposed schemes for initializing and manipulating a single electron spin in a charged exciton (trion), using self-assembled quantum dots, require polarization selective excitation of spin states.^{15,16} In nanowires, this can be achieved by directing the light along the nanowire axis.¹⁷ Thus, access to intrinsic polarization of a charge tunable nanowire quantum dot requires electrical contacts on a vertically aligned nanowire quantum dot. Here, we demonstrate single electron charging and optical readout of the polarization state by fabricating capacitively coupled surround-gates¹⁸ around as-grown nanowire quantum dots. The neutral exciton state is identified by polarization analysis of the gate voltage dependent emission lines. This charge state identification by polarization, combined with the ability to selectively excite specific spin states in the dots,¹³ shows that spin initialization and manipulation of a singly charged exciton, using the excitation polarization, is feasible in nanowire quantum dots.

The InAsP quantum dots, embedded in InP nanowires, are grown in the vapor-liquid-solid mode using metal-organic vapor-phase epitaxy.¹⁹ Growth details can be found in Ref. 13. The distance between the nanowires is larger than the spatial resolution of our optical setup ($\sim 1 \mu\text{m}$), enabling single dot excitation. Active areas are defined by op-

tical lithography and subsequent etching of nanowires outside active areas. This substrate patterning is performed postgrowth, in order to avoid effects on the quantum dot growth. A scanning electron microscope (SEM) image of an active area containing four nanowires is shown in Fig. 1(a).

As gate dielectric, 200 nm silicon oxide (SiO_2) is deposited using plasma-enhanced chemical vapor deposition. This method allows for deposition temperatures of 300 °C, preventing out-diffusion of arsenic and phosphorus. As gate metal, 15 nm titanium nitride (TiN) is sputtered onto the sample. A SEM image of a nanowire embedded in these two layers is shown in Fig. 1(b). For this figure, a 100 nm TiN layer is used to visualize the layer in SEM. A photoresist layer with a thickness exceeding the nanowire length is spun. This resist layer is etched back to the quantum dot height using an oxygen plasma. This process is depicted schematically in Fig. 1(c). The TiN layer is etched subsequently from the part of the nanowires that stick out of the resist using a CF_4 plasma. The TiN is then patterned by photolithography. Figure 1(d) shows a SEM image of a nanowire embedded in SiO_2 , and an opened (100 nm) TiN surround gate. Electrical connections are made to the gate and the wafer back side, to which a voltage difference, V_{gate} , can be applied.

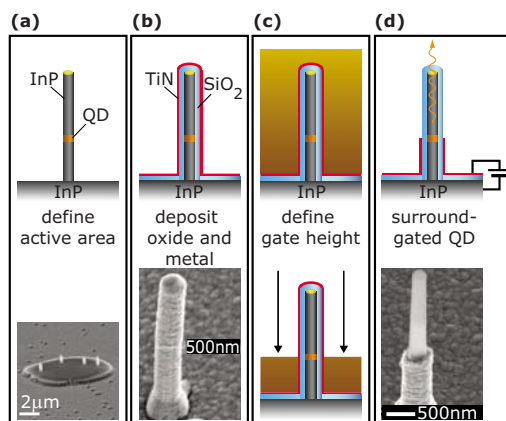


FIG. 1. (Color online) (a) Schematic of as-grown nanowire quantum dots. The SEM image shows an active area containing four nanowires. (b) Schematic and SEM image showing a nanowire covered with gate dielectric (SiO_2) and gate metal (TiN). (c) Schematics of the etch-back process defining the gate height. (d) Schematic and SEM image of the device.

^{a)}Also at Materials Innovation Institute (M2I), Delft, The Netherlands, and IMM, Solid State Chemistry, Radboud University Nijmegen, The Netherlands.

^{b)}Also at Eindhoven University of Technology, Eindhoven, The Netherlands.

^{c)}Electronic mail: v.zwiller@tudelft.nl.

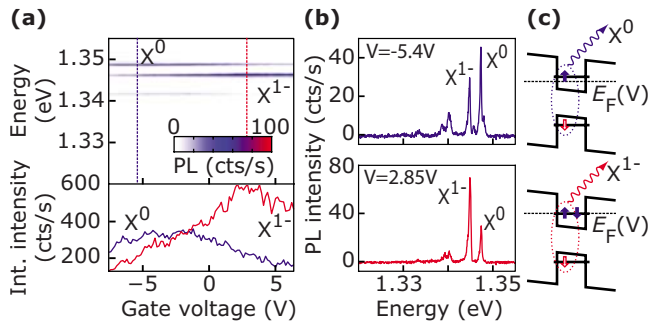


FIG. 2. (Color online) (a) Top panel shows color plot of gate voltage dependent PL spectra. Bottom panel shows integrated PL intensity of the X^0 (maximum at -5 V) and X^{1-} (maximum at 2.5 V) as function of gate voltage. (b) PL spectrum at $V_{\text{gate}} = -5.4$ V (top panel) and $V_{\text{gate}} = 2.85$ V (bottom panel). The positions of the two line cuts shown in (b) are indicated in the top panel of (a) by the two vertical dashed lines. (c) Schematic representations of the dot energy levels. By tuning the electrochemical potential E_F , the ground state contains either zero or one electron, resulting in X^0 (upper schematic) or X^{1-} (lower schematic), respectively.

Microphotoluminescence (PL) studies were performed at 4.2 K. The nanowire quantum dot devices were excited with a linearly polarized tunable titanium sapphire continuous wave laser focused to a spot size of ~ 1 μm using a microscope objective with a numerical aperture $NA = 0.65$. The PL signal was collected by the same objective and was sent to a spectrometer, which dispersed the PL onto a nitrogen-cooled silicon array detector with 30 μeV resolution. Linear and circular emission polarizations were analyzed using a half- or quarter-waveplate, respectively, followed by a fixed polarizer. Voltages were applied using battery driven voltage sources. Currents down to 10 fA could be measured.

To avoid screening of the voltage by photoexcited charges in the InP nanowire and substrate, we used quasi-resonant excitation in the p-shell ($E_{\text{exc}} = 1.36$ eV).¹³ The top panel of Fig. 2(a) shows the surround-gate voltage dependent PL spectra of the quantum dot s-shell. Figure 2(b) shows two spectra, taken at $V_{\text{gate}} = -5.4$ V (top panel) and 2.85 V (bottom panel). For gate voltages of ± 6 V or larger, a measurable leakage current (~ 20 pA) was found. At large negative gate voltages, one dominant emission line is found at 1.349 eV, assigned to the neutral exciton X^0 . The intensity of this emission line decreases by tuning the gate voltage to positive values. Simultaneously, the emission line at 1.345 eV, assigned to X^{1-} (we will motivate the assignments by polarization studies later), increases in intensity. This is seen more quantitatively in the bottom panel of Fig. 2(a), where the integrated intensities of both lines are plotted as function of gate voltage. The total added intensity of the two lines is not constant, since a third emission line appears at 1.34 eV. Also the overlap of the two emission lines is large: the two lines are visible across the whole voltage range investigated. This indicates that tunnel rates are small compared to the radiative rate. This is to be expected, since from the electric field generated, only a small component points along the nanowire axis. Hence, tunnel couplings are not changed by the surround-gate. Instead of tilting the bands, the gate induces a change in electrochemical potential E_F , as depicted schematically in Fig. 2(c). The difference in emission energy of 3 meV between X^0 and X^{1-} is due to Coulomb interaction, and corresponds very well to what is observed in similar dots,¹⁴ and to what is calculated for dots of such size.²⁰

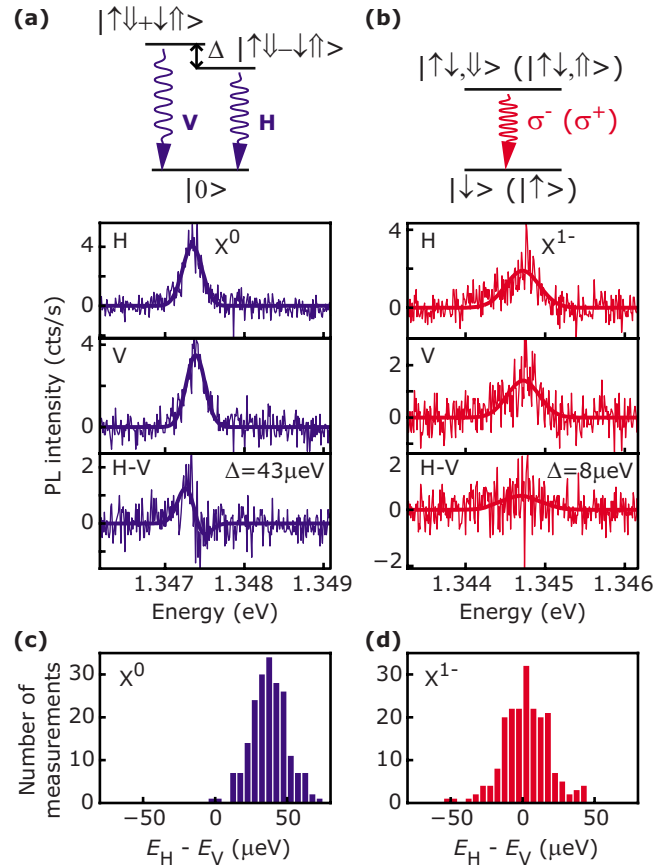


FIG. 3. (Color online) (a) Horizontal (top panel) and vertical (middle panel) polarization analysis of the neutral exciton X^0 . Lower panel shows horizontal minus vertical polarization. Thick solid lines are fits to the data (thin solid lines). (b) Similar polarization analysis as in (a) but now for the singly charged exciton X^{1-} . [(c)–(d)] Histograms of the energy differences between fits of the horizontal and vertical polarizations for (c) X^0 and (d) X^{1-} .

The assignment of the 1.349 eV emission line to neutral exciton emission X^0 is substantiated by polarization analysis. A full Stokes analysis is performed on the PL as a function of gate voltage. Figures 3(a) and 3(b) show the horizontal and vertical polarization analysis of the emission line at $E = 1.349$ eV (1.345 eV) in the top panel and the middle panel, respectively. The lower panel shows the difference of the two polarizations (horizontal minus vertical). The thick solid curves are fits to the data, used to determine the exact emission energy. In Fig. 3(a) a significant difference in emission energy for the two polarizations is observed ($\Delta = 43$ μeV), indicating a splitting due to the anisotropic exchange interaction.²¹ This interaction originates from exchange between the electron and hole spin [see energy level diagram in Fig. 3(a)]. Observation of such an anisotropic exchange splitting is a strong indication of neutral exciton emission.²²

By tuning to a more positive voltage, the emission line at 1.345 eV dominates the spectrum. This line does not show an anisotropic exchange splitting, as can be seen from Fig. 3(b). For X^{1-} no anisotropic exchange splitting is expected: the two electrons in the dot form a singlet with zero spin, resulting in vanishing exchange terms [see energy level diagram in Fig. 3(b)]. Since the double and triple charged excitons all exhibit an exchange splitting,²⁰ it can be concluded that the two dominant emission lines observed in the device originate from X^0 and X^{1-} emission. The biexciton, however, could

not be identified by polarization analysis; the emission line at 1.34 eV did not show an anisotropic exchange splitting, possibly due to the low intensity of less than one count per second; spectral diffusion might smear out the two polarization states.

An extensive polarization analysis on X^0 and X^{1-} is shown as a histogram in Fig. 3(c) for X^0 and Fig. 3(d) for X^{1-} . These statistics show that the exchange splitting in X^0 is $\Delta=40 \pm 10 \mu\text{eV}$ and $0 \pm 15 \mu\text{eV}$ for X^{1-} . The large spread in these numbers is due to the low intensity of the peaks and the relatively large spectral diffusion: linewidths are about $200 \mu\text{eV}$. The magnitude of the X^0 splitting is comparable to what is usually found in self-assembled dots but rather unexpected, since nanowire quantum dots are believed to be highly symmetric.²³ Nonuniform strain, induced by the surrounding oxide could result in an enhanced anisotropic exchange interaction. No effect of the gate voltage on the magnitude of the anisotropic exchange splitting of X^0 has been observed.

In conclusion, we have fabricated quantum dots in vertically aligned, surround-gated nanowires, crucial for accessing the polarization properties of the dots. These devices show single electron charging. The neutral X^0 and singly charged X^{1-} excitons are identified by polarization analysis. These results demonstrate that quantum dots in vertical nanowire devices are promising for single electron spin manipulation by means of electron spin to polarization coupling.

We acknowledge W. van den Einden, A. Helman, and G. Immink for help and fruitful discussions. This work was supported by the European FP6 NODE (Grant No. 015783) project, the Dutch Organization for Fundamental Research on Matter (FOM), The Netherlands Organization for Scientific Research (NWO), and the Dutch ministry of economic affairs (NanoNed). The work of R.E.A. was carried out under Project No. MC3.0524 in the framework of the strategic research program of the Materials Innovation Institute (M2I) (www.m2i.nl).

¹P. Michler, A. Kiraz, C. Becher, W. V. Schoenfeld, P. M. Petroff, L. Zhang, E. Hu, and A. Imamoglu, *Science* **290**, 2282 (2000).

- ²N. Akopian, N. H. Lindner, E. Poem, Y. Berlatzky, J. Avron, D. Gershoni, B. D. Gerardot, and P. M. Petroff, *Phys. Rev. Lett.* **96**, 130501 (2006).
- ³A. Hartmann, Y. Ducommun, E. Kapon, U. Hohenester, and E. Molinari, *Phys. Rev. Lett.* **84**, 5648 (2000).
- ⁴N. Gisin and R. Thew, *Nat. Photonics* **1**, 165 (2007).
- ⁵M. Atatüre, J. Dreiser, A. Badolato, A. Högele, K. Karrai, and A. Imamoglu, *Science* **312**, 551 (2006).
- ⁶B. D. Gerardot, D. Brunner, P. A. Dalgarno, P. Öhberg, S. Seidl, M. Kroner, K. Karrai, N. G. Stoltz, P. M. Petroff, and R. J. Warburton, *Nature (London)* **451**, 441 (2008).
- ⁷J. Berezovsky, M. H. Mikkelsen, N. G. Stoltz, L. A. Coldren, and D. D. Awschalom, *Science*, **320**, 349 (2008).
- ⁸D. Press, T. D. Ladd, B. Zhang, and Y. Yamamoto, *Nature (London)* **456**, 218 (2008).
- ⁹C. M. Lieber and Z. L. Wang, *MRS Bull.* **32**, 99 (2007).
- ¹⁰M. T. Borgström, V. Zwiller, E. Muller, and A. Imamoglu, *Nano Lett.* **5**, 1439 (2005).
- ¹¹E. D. Minot, F. Kelkensberg, M. van Kouwen, J. A. van Dam, L. P. Kouwenhoven, V. Zwiller, M. T. Borgström, O. Wunnicke, M. A. Verheijen, and E. P. A. M. Bakkers, *Nano Lett.* **7**, 367 (2007).
- ¹²C. Fasth, A. Fuhrer, M. T. Björk, and L. Samuelson, *Nano Lett.* **5**, 1487 (2005).
- ¹³M. H. M. van Weert, N. Akopian, U. Perinetti, M. P. van Kouwen, R. E. Algra, M. A. Verheijen, E. P. Bakkers, L. P. Kouwenhoven, and V. Zwiller, *Nano Lett.* **9**, 1989 (2009).
- ¹⁴M. P. van Kouwen, M. E. Reimer, A. W. Hidma, M. H. M. van Weert, R. E. Algra, E. P. A. M. Bakkers, L. P. Kouwenhoven, and V. Zwiller, *Nano Lett.* **10**, 1817 (2010).
- ¹⁵A. Shabaev, A. L. Efros, D. Gammon, and I. A. Merkulov, *Phys. Rev. B* **68**, 201305 (2003).
- ¹⁶O. Gywat, H.-A. Engel, D. Loss, R. J. Epstein, F. M. Mendoza, and D. D. Awschalom, *Phys. Rev. B* **69**, 205303 (2004).
- ¹⁷M. H. M. van Weert, N. Akopian, F. Kelkensberg, U. Perinetti, M. P. van Kouwen, J. Gómez Rivas, M. T. Borgström, R. E. Algra, M. A. Verheijen, E. P. A. M. Bakkers, L. P. Kouwenhoven, and V. Zwiller, *Small* **5**, 2134 (2009).
- ¹⁸H. T. Ng, J. Han, T. Yamada, P. Nguyen, Y. P. Chen, and M. Meyyappan, *Nano Lett.* **4**, 1247 (2004).
- ¹⁹K. Hiruma, T. Katsuyama, K. Ogawa, M. Koguchi, H. Kakibayashi, and G. P. Morgan, *Appl. Phys. Lett.* **59**, 431 (1991).
- ²⁰M. Ediger, G. Bester, A. Badolato, P. M. Petroff, K. Karrai, A. Zunger, and R. J. Warburton, *Nat. Phys.* **3**, 774 (2007).
- ²¹M. Bayer, G. Ortner, O. Stern, A. Kuther, A. A. Gorbunov, A. Forchel, P. Hawrylak, S. Fafard, K. Hinzer, T. L. Reinecke, S. N. Walck, J. P. Reithmaier, F. Klopff, and F. Schäfer, *Phys. Rev. B* **65**, 195315 (2002).
- ²²E. Poem, J. Shemesh, I. Marderfeld, D. Galushko, N. Akopian, D. Gershoni, B. D. Gerardot, A. Badolato, and P. M. Petroff, *Phys. Rev. B* **76**, 235304 (2007).
- ²³R. Singh and G. Bester, *Phys. Rev. Lett.* **103**, 063601 (2009).